

Visible range whispering-gallery mode in microdisk array based on size-controlled Si nanocrystals

Rong-Jun Zhang,^{a)} Se-Young Seo, Alexey P. Milenin, Margit Zacharias,^{b)} and Ulrich Gösele

Max-Planck-Institute of Microstructure Physics, Weinberg 2, 06120 Halle, Germany

(Received 8 November 2005; accepted 20 March 2006; published online 13 April 2006)

Microdisks based on in-plane embedded size-controlled Si nanocrystal/SiO₂ superlattices (Si-NCs/SiO₂ SLs) were mass-fabricated arranged in well-ordered arrays. The microdisks were fabricated with size irregularity of below 0.2% over large-scale areas. Overlapping whispering-gallery modes (WGM) of the visible nanocrystalline-silicon luminescence were observed. A comparison between analytical calculation and experimental results is reported. We found that only one axial and one radial WGM exist due to their thin disk thickness and birefringence characteristic of Si-NCs/SiO₂ SLs, and that the mode spacing is 15 nm and 6 nm for microdisks with a diameter of 8.8 μm and 23.7 μm, respectively. The advantages of such size-controlled Si-NCs/SiO₂ embedded in microdisk arrays for Si-based photonic application will be discussed. © 2006 American Institute of Physics. [DOI: 10.1063/1.2195712]

Optical microdisks, which confine light to a small modal volume by resonant recirculation with low optical loss, have received considerable attention during the past years. Si-based microphotonic devices have been a technical challenge with respect to mass production of highly integrated photonic devices with the help of present mature complementary metal-oxide-semiconductor technique.¹ Photonic devices based on Si are expected at least partially to functionally replace the present electronic devices. As novel examples of Si-based integrated photonic devices, the silicon optical modulator and silicon Raman laser have been reported so far.²⁻⁴ In past decades, the efficient visible luminescence at room temperature from silicon nanocrystals (Si-NCs) was a focus of interest because it might lead to the development of a Si-based efficient light source.^{5,6} Recently, optical gain in Si-NCs, and a electroluminescent field-effect device based on Si-NCs, were demonstrated.^{7,8}

In order to further decrease the overall size of a Si-NC-based light source, more efficient device structures need to be adopted. One candidate for such a structure is the microdisk resonator, which has an excellent Q value and many advantages for lasing which is realized by nearly infinite light circulations of whispering-gallery modes (WGMs) within a small volume.⁹ Even though a high- Q value and lasing were already observed from silica microdisks,^{10,11} little has been reported demonstrating whispering-gallery modes of the visible luminescence from Si-NCs in a microdisk.¹²

In this letter, we present the mass fabrication of microdisk based on Si-NCs in an arrayed structure, and the observation of WGMs from them. We will show the clear emergence of WGMs in microdisk arrays.

The preparation of multilayers of size-controlled Si-NCs in SiO₂ matrix was reported elsewhere.¹³ As a first step, a 50 nm buffer SiO₂ layer was evaporated on Si(100) wafers. Then, 30 periods of the SiO_x/SiO₂ superlattices (SLs) were evaporated on top as the active emitting part of

the microdisk. The thickness of the SiO_x and SiO₂ layers was 3 nm and 4 nm, respectively. Finally, an additional 50 nm buffer SiO₂ layer was added to protect the layered structure. The total film thickness including the top/bottom SiO₂ layers is about 310 nm. The samples were then annealed at 1100 °C for 1 h under a N₂ atmosphere to realize the Si-NCs in the SiO₂ matrix.

Optical lithography was used to pattern various structures. The etching processes were undertaken using sequential anisotropic and isotropic dry plasma etching processes. Thus, while the *c*-C₄F₈/90% Ar plasma chemistry was used to etch anisotropically through the SiO₂ layer with the embedded Si-NCs, the SF₆ plasma was used to etch isotropically the Si substrate.¹⁴

Finally, arrays of microdisks with diameters of 8.8 μm, 23.7 μm, and 48.0 μm were achieved. For comparison, an array of microsquares with a side length of 8.8 μm was also prepared. The microdisks were arranged in a hexagonal array with side length of 13, 28, and 55 μm, depending on the size of the microdisks with 8.8 μm, 23.7 μm, and 48.0 μm diameter, respectively. For the microsquares arrays, we chose a square lattice arrangement, with a lattice constant of 12.5 μm. As a result, the peripheries of microdisks or microsquares were separated from their neighboring ones by at least ~4 μm, ensuring a sufficient separation to effectively exclude optical coupling between microdisks or microsquares.

Room-temperature photoluminescence (PL) was measured using liquid-nitrogen-cooled charge-coupled-device camera attached to a single monochromator. The 488 nm line of an Ar laser with a power density of 6 W/cm² was used as excitation source. The Si-NCs/SiO₂ SL of an unstructured part, and the arrays of microdisks or microsquares were measured under the same conditions. All spectra were corrected for the wavelength depending sensitivity of the measuring system. Scanning electron microscopy (SEM) was performed using a JSEM 6300F.

Figure 1(a) shows the SEM image of an array of microdisks with a diameter of 8.8 μm. The hexagonal arrangement of the microdisks can clearly be seen. No defective/misshaped disk was found by the SEM investigation over the

^{a)}Present address: Department of Optical Science and Engineering, Fudan University, Shanghai 200433, China.

^{b)}Electronic mail: zacharia@mpi-halle.de

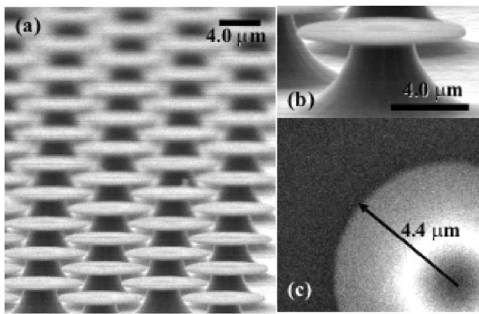


FIG. 1. SEM images of (a) the microdisk array. The microdisks are about 310 nm thick and have a diameter of 8.8 μm. (b) A selected single-microdisk resonator consisting of the thin silica layer with the embedded Si-NCs/SiO₂ SL upon a Si post and the Si substrate. (c) Top view.

scanned area. In Fig. 1(b), a single microdisk is shown. The periphery of the microdisk shows a uniform undercut. The thin asymmetric trunk below the microdisk is the etched single-crystalline Si of the wafer substrate. In Fig. 1(c), a selected top view of one microdisk is presented (white circular area) demonstrating the very smooth microdisk edge. The SEM results for other diameters and for the microsquare arrays are as smooth as the presented microdisk in Fig. 1.

Figure 2(a) compares the room-temperature PL spectra of the unstructured bare film, the microdisk array, and the microsquare array. All of the spectra show the similar luminescence profiles peaked at 800 nm which is typical observed from Si-NCs with a diameter of 3 nm. While no notable features are found for the spectra of the unstructured film and the microsquare array, the spectra of the microdisk array show small peaks superimposed on the luminescence

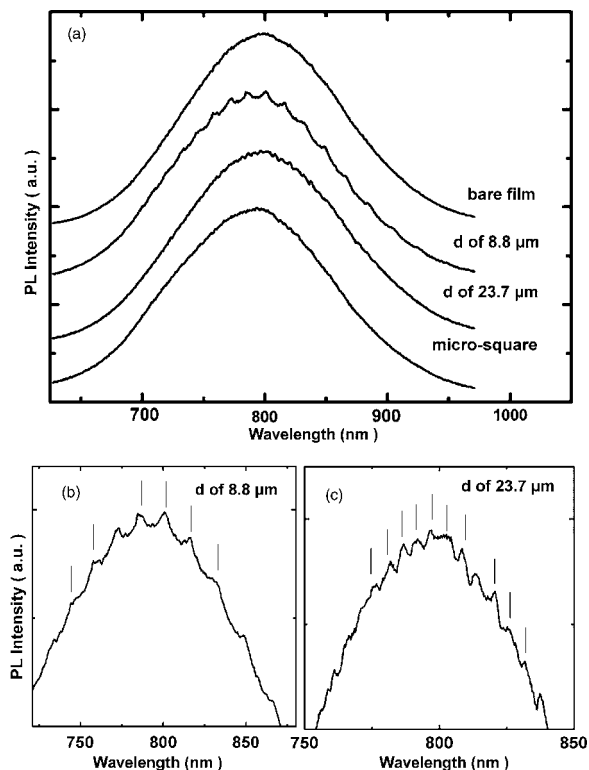


FIG. 2. PL measurements of (a) a Si-NCs/SiO₂ SL unstructured bare film, the array of microdisks with a diameter of 8.8 μm and 23.7 μm, and the array of microsquares with a square length of 8.8 μm. (b) Enlarged view for the array of microdisks with a diameter of 8.8 μm. (c) The microdisks with a diameter of 23.7 μm.

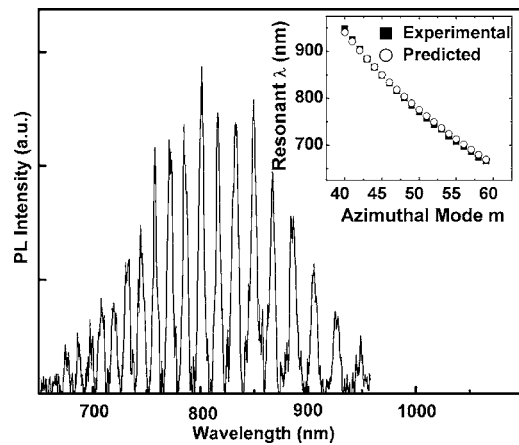


FIG. 3. WGMs emission deduced from PL measurements. Inset: Comparison of experimental results and predicted data for the resonant peaks via azimuthal mode number.

of the Si-NCs, as shown in the enlarged spectra [Figs. 2(b) and 2(c)].

Such sigmoid luminescence peaks can result from the optical interference within a film or the interference between direct luminescence from disk and its reflected luminescence at a substrate, or can be the radial guiding mode in a microstructure.¹⁵ However, we can exclude these possibilities, because they would appear in the PL spectra of the unstructured SL film or of the microsquare array, too.

Instead, those narrow peaks superimposed on the spontaneous emissions of Si-NCs can be attributed to WGMs in the microdisks. The spacing between two neighboring peaks is almost the same for each spectrum; and the average spacing decreases as the diameter of the microdisk increases. These results are typically expected for WGMs of a microdisk. Moreover, the fact that we did not observe such peaks from the microdisks with a diameter of 48.0 μm (not shown) is also consistent, because here the expected spacing is ~3 nm, which is too narrow to be resolved under the measurement conditions used. Figure 3 shows the WGMs emission of an array of microdisks with diameter of 8.8 μm, after deduction of Si-NCs spontaneous luminescence as background from the overall PL spectrum in Fig. 2(b). Now, the resonance peaks can be clearly observed.

The WGMs within a disk can be understood by a complete solution of the three-dimensional Maxwell equations using cylindrical coordinates. Since such a full analysis of WGMs within a microdisk is rather complicated, we tried to analyze them with a rather simple model as follows: First, because the thickness of the microdisk is less than $\lambda/2n_{\text{eff}}$, where λ and n_{eff} is the vacuum wavelength and the effective refractive index of the disk, respectively, only one fundamental transverse electric (TE) and transverse magnetic (TM) axial mode can exist.^{16,17} In addition, we recently observed that the birefringence behavior from our nc-Si/SiO₂ SLs, due to the anisotropic layered film structure and the optical filling factor of the TE mode, is much higher than that of the TM mode.¹⁸ This fact implies that the coupling of the TE mode to microdisk is dominant over the TM mode, and it can be assumed that the observed modes mostly originate from the TE mode. Then, we can simplify the problem to two-dimensional equations with a polar coordinate. Based on the solution of the two-dimensional Helmholtz equation, the field distribution $\psi(r, \theta)$ is¹⁶

$$\psi(r, \theta) \sim J_{m,n}(2\pi n_{\text{eff}}r/\lambda_{\text{res}})e^{im\theta}, \quad (1)$$

where r and θ are polar coordinates, $J_{m,n}$ are Bessel functions, and m and n are the azimuthal mode and the radial mode number, respectively. λ_{res} is the resonant wavelength. For the effective refractive index n_{eff} , we used 1.60 for the TE₀ mode considering the light confinement in a slab waveguide. The high refractive index contrast between the film and the air, and the spatial difference between the disk diameter and resonance wavelength, allow us to assume that WGMs are strongly confined within a disk and the field intensity is almost zero at the disk radius R ,^{19,20} setting the boundary condition to be $J_{m,n}(2\pi n_{\text{eff}}R/\lambda_{\text{res}}) = 0$. In fact, this approximation has been successfully used in the case of semiconductor microdisks.^{19,20} Finally, we can find resonance wavelengths of WGMs and their corresponding mode numbers. In the case of the microdisk with a diameter of 8.8 μm , the azimuthal mode number was found to range from $m=40$ (for $\lambda_{\text{res}}=950$ nm) to 60 (for $\lambda_{\text{res}}=650$ nm) in the spectral range of Fig. 3 for the first radial mode. Experimental peaks can be assigned to the TE_{0 m ,1} modes with azimuthal modes, with a mode spacing of ~ 15 nm, in good agreement with the calculation as shown in the inset of Fig. 3. The second or higher orders can not be matched with the experimental results. So, only the first-order radial modes, the TE_{0 m ,1} modes, can be observed in our microdisk array. Similarly, for the array of microdisks with a disk diameter of 23.7 μm , we observed only first-order radial modes. Due to the absence of both higher axial modes and higher radial modes, the resonance peak spacing is determined only by azimuthal modes. As a result, the mode spacing is 15 nm and 6 nm, and rather broad for microdisks with a diameter of 8.8 μm and 23.7 μm , respectively. This fact has important implications since broader mode spacing is more advantageous for the development of a single-line light source.

The resonant peaks in the PL spectrum result from the overlapping of individual modes from each microdisk since PL measurements were performed by pumping several thousands of microdisks at the same time. Thus, the Q factor, which can be evaluated from Fig. 3, is mainly determined by slight irregularities in disk diameter rather than the effect of the roughness of the periphery. Using higher resolved PL measurements with a resolution of 0.4 nm, a full width at half maximum at each resonant mode was observed to be 2 nm. Thus, the Q factor of the microdisk array was calculated to be around 400 for microdisks with a diameter of 8.8 μm . While this Q value seems to be much smaller than reported value for a silica-based microdisk,¹⁰ to the contrary, this result implies the excellent mass fabrication of microdisks with a size deviation of $<0.2\%$ between each microdisk, since 1% of the diameter deviation would limit the overall Q factor of the microdisk array to below 80.

In addition to the excellent mass production and the observation of WGMs of the Si-NCs microdisk array, it is worth noting the advantage of size-controlled Si-NC/SiO₂ SLs as a base material for the microdisks compared to other conventional Si-NCs methods.²¹ For microphotonic devices, which are based on Si-NCs for active optical emission, both the Si-NC size—which determines the luminescence properties, and the film refractive index—which influences the character of WGMs, are important parameters. However, the size distribution of Si-NCs is fairly broad for conventional Si-NCs in a SiO₂ matrix, which are generally formed by

high-temperature anneals of amorphous SiO_x ($a\text{-SiO}_x$) films fabricated by chemical vapor deposition, sputtering, or ion-implantation of Si ions. This wider size distribution of Si-NCs is disadvantageous for laser applications. In contrast, the size distribution of Si-NCs in our SLs is rather narrow.¹³ Second in order to design microdisks flexibly for optimal operation, independent control of the Si-NCs size and the refractive index is required at the same time. For our SiO_x/SiO₂ SLs, the Si-NC size and the refractive index can be independently controlled and designed quite well. Finally, the birefringence behavior of SiO_x/SiO₂ SLs film allows the selective coupling of TE modes, rather than TM modes, to the microdisk, inducing wider mode spacing.

In conclusion, we presented microdisk resonators which are based on size-controlled Si-NCs in a SiO₂ matrix. The mass production of such microdisk resonators in large-scale arrays was demonstrated. WGMs, from the visible luminescence of Si-NCs, were observed for the microdisk array. Thin layer thickness and the birefringence of SLs films allow one to sustain only one axial and one radial mode; inducing a rather broad mode spacing of up to 15 nm. The used process technology for the integration of microdisks is compatible with planar silicon-process technology. We expect that such microdisk arrays can be applied as a base material for integrated Si microphotronics.

R.J.Z. gratefully acknowledges financial support from the Alexander von Humboldt Foundation. S.Y.S. gratefully acknowledges financial support from the Korea Research Foundation.

¹*Towards the First Silicon Laser*, NATO Science Series, edited by L. Pavesi, S. Gaponenko, and L. Dal Negro (Kluwer, Dordrecht, 2003).

²Q. F. Xu, B. Schmidt, S. Pradhan, and M. Lipson, *Nature (London)* **435**, 325 (2005).

³A. S. Liu, R. Jones, L. Liao, D. Samara-Rubio, D. Rubin, O. Cohen, R. Nicolaescu, and M. Paniccia, *Nature (London)* **427**, 615 (2004).

⁴H. Rong, A. Liu, R. Jones, O. Cohen, R. Nicolaescu, A. Fang, and M. Paniccia, *Nature (London)* **433**, 292 (2005).

⁵W. L. Wilson, P. F. Szajowski, and L. E. Brus, *Science* **262**, 1242 (1993).

⁶J. Heitmann, F. Müller, L. X. Yi, M. Zacharias, D. Kovalev, and F. Eichhorn, *Phys. Rev. B* **69**, 195309 (2004).

⁷L. Pavesi, L. D. Negro, C. Mazzoleni, G. Franzo, and F. Priolo, *Nature (London)* **408**, 440 (2000).

⁸R. J. Walters, G. I. Bourianoff, and H. A. Atwater, *Nat. Mater.* **4**, 143 (2005).

⁹K. J. Vahala, *Nature (London)* **424**, 839 (2003).

¹⁰T. J. Kippenberg, S. M. Spillane, D. K. Armani, and K. J. Vahala, *Appl. Phys. Lett.* **83**, 797 (2003).

¹¹X. Liu, W. Fang, Y. Huang, X. H. Wu, S. T. Ho, H. Cao, and R. P. H. Chang, *Appl. Phys. Lett.* **84**, 2488 (2004).

¹²D. S. Gardner and M. L. Brongersma, *Opt. Mater. (Amsterdam, Neth.)* **27**, 804 (2005).

¹³M. Zacharias, J. Heitmann, R. Scholz, U. Kahler, M. Schmidt, and J. Blaessing, *Appl. Phys. Lett.* **80**, 661 (2002).

¹⁴A. P. Milenin, C. Jamois, T. Geppert, U. Gösele, and R. B. Wehrspohn, *Microelectron. Eng.* **81**, 15 (2005).

¹⁵H. J. Moon, Y. T. Chough, and K. An, *Phys. Rev. Lett.* **85**, 3161 (2000).

¹⁶S. L. McCall, A. F. J. Levi, R. E. Slusher, S. J. Pearton, and R. A. Logan, *Appl. Phys. Lett.* **60**, 289 (1992).

¹⁷R. E. Slusher, A. F. J. Levi, U. Mohideen, S. L. McCall, S. J. Pearton, and R. A. Logan, *Appl. Phys. Lett.* **63**, 1310 (1993).

¹⁸D. Navarro-Urrios, F. Riboli, M. Cazzanelli, A. Chiasera, N. Daldosso, L. Pavasi, C. J. Oton, J. Heitmann, L. X. Yi, R. Scholz, and M. Zacharias, *Opt. Mater. (Amsterdam, Neth.)* **27**, 763 (2005).

¹⁹X. Liu, W. Fang, Y. Huang, X. H. Wu, S. T. Ho, H. Cao, and R. P. H. Chang, *Appl. Phys. Lett.* **84**, 2488 (2004).

²⁰N. C. Frateschi and A. F. J. Levi, *Appl. Phys. Lett.* **66**, 2932 (1995).

²¹J. Heitmann, F. Müller, M. Zacharias, and U. Gösele, *Adv. Mater. (Weinheim, Ger.)* **17**, 795 (2005).